Article

INTERNATIONAL JOURNAL OF DAMAGE MECHANICS

International Journal of Damage Mechanics
2014, Vol. 23(4) 523–536

DOI: 10.1177/1056789513501683
ijd.sagepub.com

SAGE

The influence of rolling speed on the fatigue life of rolls with grooves

Željko Domazet[1], Francisko Lukša[1] and Tatjana Stanivuk[2]

Abstract

In the hot rolling process, rolls with grooves are used for the production of various simple and complex profiles. Main factors influencing the fatigue life of these rolls result from the technological process of the rolling. Rolling speed is an important parameter of technological process which has great influence on overall production. In order to increase rolling production, an analysis of the rolling speed influence on the fatigue life of the rolls has been carried out. The fatigue life estimation is carried out according to the fatigue life stress concept based on the local stress. Stress spectra in critical areas are determined for three different roll speeds. The analysis shows that although increasing the rolling speed causes decrease of the fatigue life of the roll, the stresses caused by the rolling at the highest speed should not lead to roll fracture.

Keywords

Fatigue, fatigue life, shape rolling, rolls with grooves, rolling speed

Introduction

In hot rolling, the rolling speed is an important parameter of technological process and overall production depends on the rolling speed. Many producers want to increase the capacity of existing production line. One of the ways to increase the rolling mill production is to increase the rotation speed of existing rolling mill stands which can affect the roll fatigue life (Lukša, 2013). In order to increase the rolling production and to avoid possible fatigue failure of the rolls (Domazet et al., 2007),

[1]Faculty of Electrical Engineering, Mechanical Engineering and Naval Architecture, University of Split, Ruđera Boškovića, Split, Croatia
[2]Faculty of Maritime Studies, University of Split, Zrinsko-Frankopanska, Split, Croatia

Corresponding author:
Francisko Lukša, Faculty of Electrical Engineering, Mechanical Engineering and Naval Architecture, University of Split, Ruđera Boškovića 32, Split 21000, Croatia.
Email: francisko.luksa@st.t-com.hr

an analysis of the rolling speed influence on fatigue life of the rolls has been carried out on three-high-roughing mill stand in ''Steelworks Split''. Additional motivation for this study was the lack of adequate literature.

Three-high-roughing mill stand was suitable for hot rolling of the billets with initial cross-section 100 mm square and 3 m initial length in eighth passes. The rolling mill production was 70 billets per hour. The mass of one billet was 230 kg. The rolling material was reinforcement steel mark BSt (Betonstahl) 400 S according to German standard Deutsches Institut für Normung (DIN) 488. The initial temperature of the rolled material in the first pass was 1200°C. The roll speed was 120 r/min. The total length of the roll was 2300 mm, the roll barrel length was 1400 mm and the roll barrel diameter was 450 mm. The material used for the rolls was nodular graphite cast iron with the pearlitic base with hardness on the roll surface 380 HB. The roll machining due to wearing was estimated after 4000 rolling tons of steel.

Figure 1 shows the roll design and groove distribution (designs and technological rules Steelworks Split). Pass shape rolling sequence (pass schedule) between rolls and corresponding grooves is numbered. The pass schedule and corresponding data are shown in Table 1.

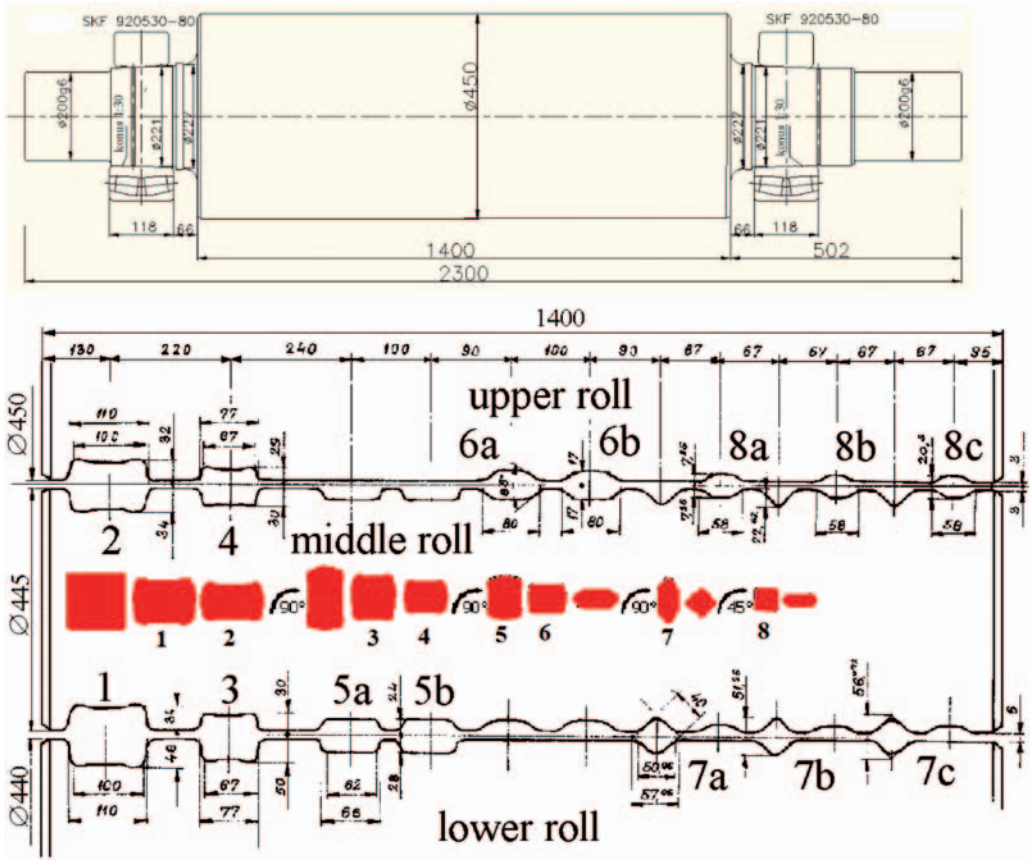

Figure 1. Roll design, groove distribution and rolling sequence.

Table 1. Pass schedule.

Pass		1	2	3	4	5	6	7	8
Pass shape		Box	Box	Box	Box	Box	Oval	Square	Oval
Groove dimensions (mm)		100 × 82	100 × 66	67 × 80	67 × 59	66 × 52	80 × 34	40	58 × 20
Cross-section (mm^2)	9850	8015	6474	5398	4032	3280	2286	1578	1075
Width (mm)	100	104	108	71	76	65	82.5	53.5	60.5
Initial height (mm)		100.0	82.0	108.0	80.0	76.0	52.0	82.5	40.0
Height after pass (mm)		82.0	66.0	80.0	59.0	52.0	34.0	51.0	20.5
Average draught (mm)		17.6	14.3	15.2	18.0	11.6	12.0	13.2	8.3
Absolute reduction (mm^2)		1835	1541	1076	1366	752	994	708	503
Elongation coefficient		1.23	1.24	1.20	1.34	1.23	1.43	1.45	1.47
Working diameter (mm)		372.5	393.5	372.5	398.5	396.5	419.5	397.25	433
Roll speed (r/min)		120	120	120	120	120	120	120	120
Length of rolled stock (m)	3	3.69	4.56	5.47	7.33	9.01	12.93	18.73	27.49
Projected length of arc of contact (mm)		57.84	56.10	72.08	64.68	68.97	61.44	79.10	64.97
Projected area of contact (mm^2)		5900	5947	4938	4754	4276	4531	3461	3265
Rolling speed (ms^{-1})		2.33	2.62	2.42	2.77	2.55	2.78	2.7	2.89
Rolling time (s)		1.58	1.74	2.26	2.65	3.53	4.65	6.92	9.52
Pause (s)		3	3	3	3	3	3	3	3
Pull through angle – α (°)		18.1	16.6	22.9	19.9	20.4	17	23.5	17.5
Deformation speed (s^{-1})		7.9	9.5	7.4	12	9.6	15.5	10.5	18.7

Rolling speed limit

Increase in the rolling speed is limited by the pull through angle. Pull through angles in the passes are determined in accordance with relation (Čaušević, 1983):

$$\alpha = \arcsin(2l_d/D), \tag{1}$$

where l_d is projected length of arc of contact and D is diameter of the roll. Pull through angles in the passes are shown in Table 1. From the comparison of the pull through angles shown in Table 1, it can be seen that the biggest pull through angle is 23.5° in the pass 7.

Experimentally obtained diagram of Z. and R. Wusatowski (Čaušević, 1979), shown in Figure 2 is used for the estimation of maximum rolling speed.

From Figure 2 it is visible that the maximum rolling speed for pull through angle of 23.5° is $4\,ms^{-1}$, which is 1.5 time more than the rolling speed in seventh pass, see Table 1. According to that, maximum possible increase in roll speed is from 120 to 180 r/min. The increase in roll speed from 120 to 150 r/min and 180 r/min is analysed.

Resistance to deformation

The main parameter in describing the rolling force is resistance to deformation of rolling material. Resistance to deformation depends on the rolling temperature, deformation speed

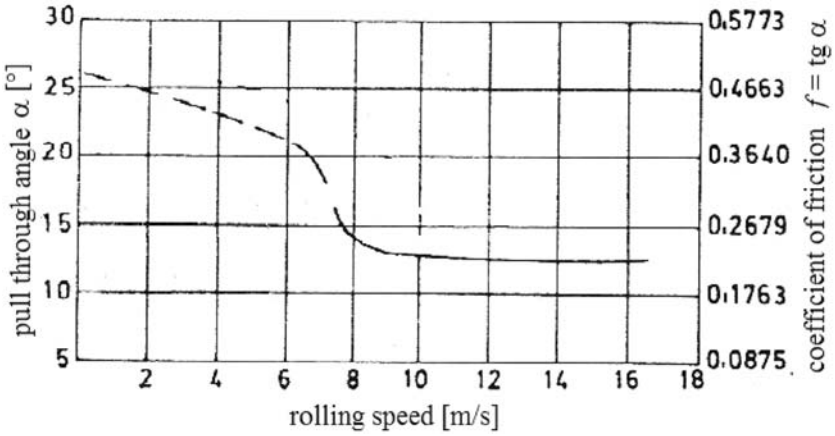

Figure 2. Pull through angle of low carbon steel with 0.18% C, Z. & R. Wusatowski.

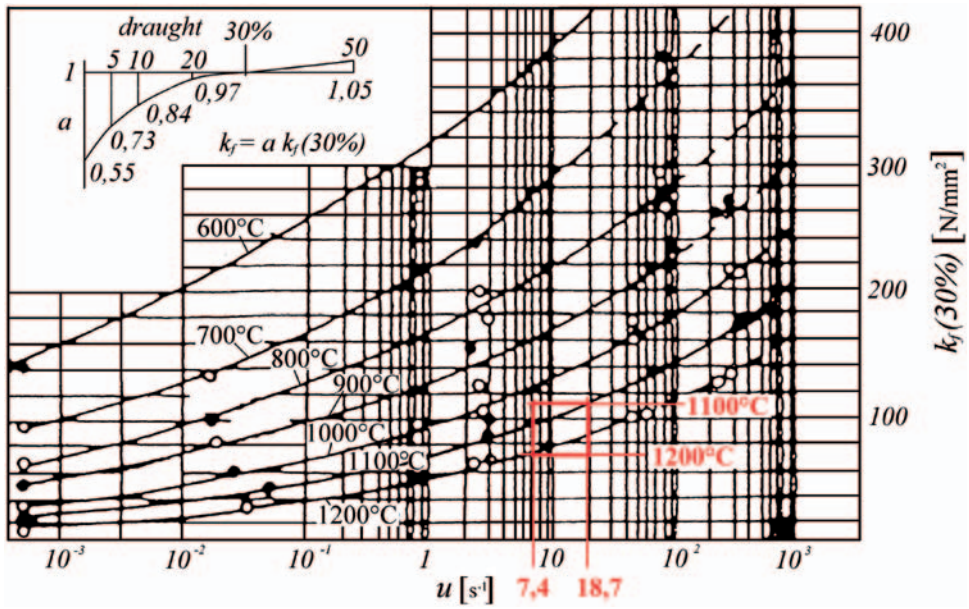

Figure 3. Resistance to deformation of low carbon steel St3, Dinnik.

and deformation size. Figure 3 shows experimentally obtained diagram of Dinnik (Čaušević, 1979), deformation resistance of low carbon steel St3 for the draught of 30% and different deformation speed and rolling temperature. For draught different than 30%, value of resistance to deformation from this diagram should be multiplied by correction factor a (curve on top of the same diagram).

For rolling sequence in 8 passes on three-high-roughing mill stand, deformation speed is in the range between 7.4 and 18.7 s^{-1}, see Table 1, and rolling temperature is in the range between 1200 and 1100°C (Figure 3). Initial temperature in the first pass was 1200°C. The drop in rolling

Table 2. Experimentally determined rolling forces.

Pass	1	2	3	4	5	6	7	8
Rolling temperature (°C)	1200	1198	1194	1188	1183	1176	1169	1159
Experimentally determined rolling forces (kN)	356.1	494.6	356.1	524.2	346.2	544.0	286.8	445.1

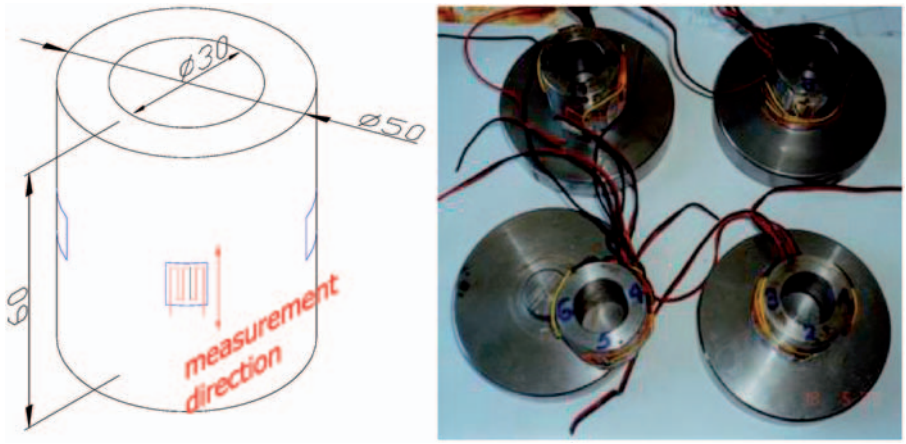

Figure 4. Load cells.

temperature was monitored using digital pyrometer, see Table 2. Temperature in eighth pass was 1148°C.

Deformation speeds are determined in accordance with the relation (Čaušević, 1983):

$$u = \frac{2v}{h_0 + h_1}\sqrt{\frac{2\Delta h_{sr}}{R_1 + R_2}} \tag{2}$$

where v is rolling speed, h_0 is initial height and h_1 is height after pass, Δh_{sr} is average draught and R_1 and R_2 are radiuses of rolls.

Stress spectrum determination

Since there are numerous formulae for calculating the rolling force in hot rolling (Čaušević, 1979), analytical calculation for this process was done according to methods of Tselikov, Ekelund, Korolev, Geleji, Golovin and Tiagunov, Sims and Siebel and the results were compared (Lukša, 2005). Comparison of the results shown large deviations, see Figure 6. Therefore, the rolling forces were determined by experimental testing (Domazet and Lukša, 2005).

In accordance with the results from analytical methods for determining the rolling force, four load cells, with three strain gauges on each, were designed for experimental determining of the rolling force (Figure 4).

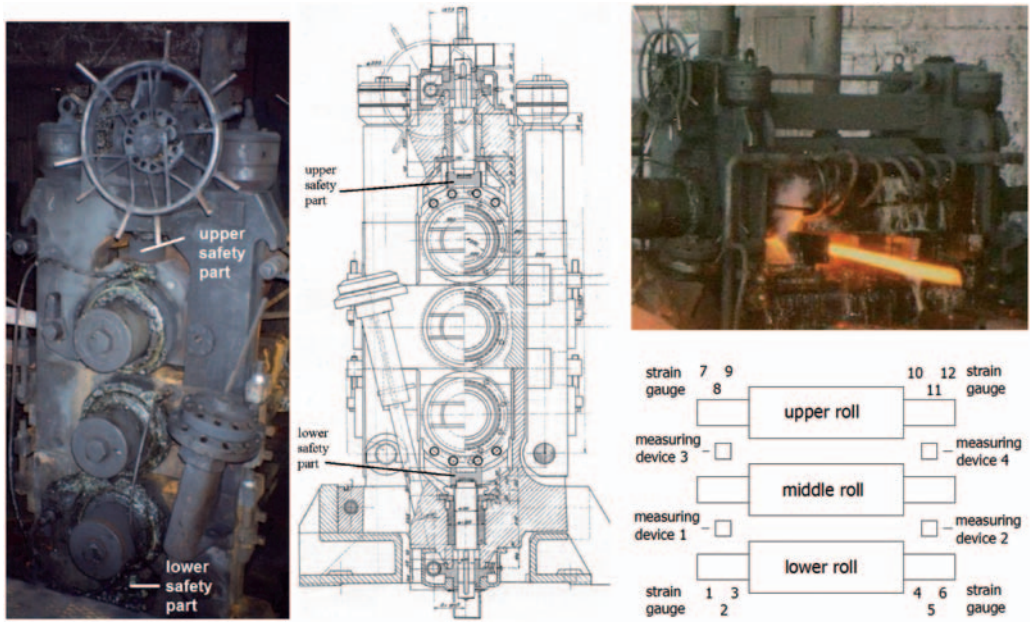

Figure 5. Positions of the load cells on three-high-roughing mill stand.

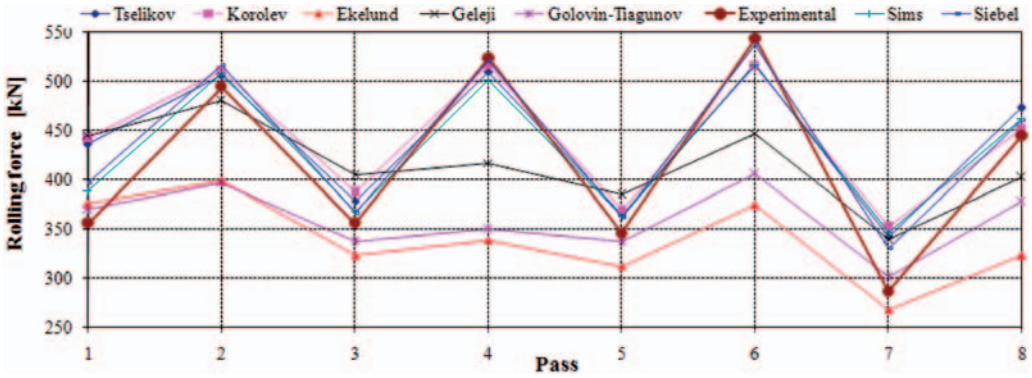

Figure 6. Analytically and experimentally determined rolling forces.

The measuring devices were mounted on both sides of the stand, instead of two safety parts against the breakage of rolls (Figure 5). One pair of load cells was used to measure reaction forces due to rolling force between two rolls (lower and middle roll or middle and upper roll). Measurement of rolling forces was carried out during the 1 h of rolling production.

Experimentally determined rolling forces are shown in Table 2. Figure 6 shows the comparison of experimentally determined rolling forces and calculated results according to methods of Tselikov, Ekelund, Korolev, Geleji, Golovin and Tiagunov, Sims and Siebel for rolling in eight passes, see Table 1 and Figure 1.

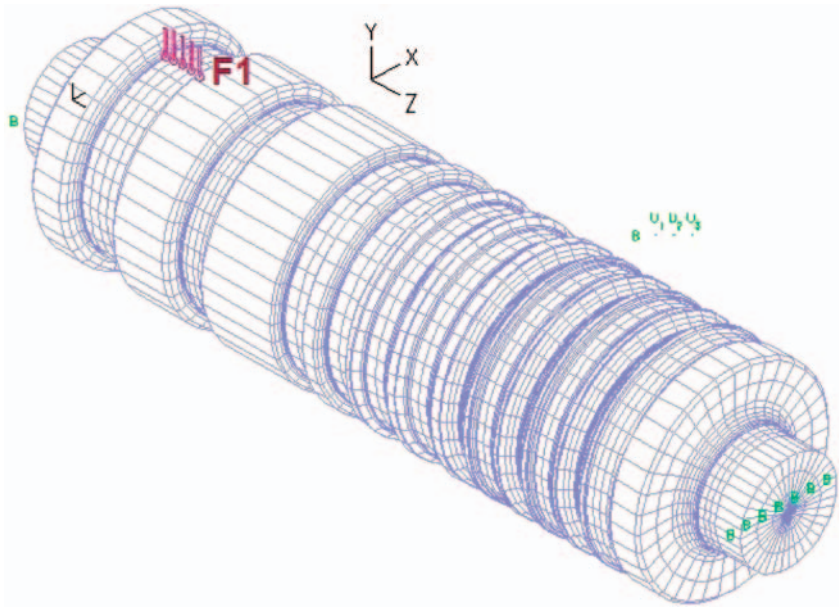

Figure 7. Linear elastic model with 3D solid elements.

It may be seen from the curves shown in Figure 6 that, for the same rolling conditions, there are large deviations in the calculated values of force rolling by different authors. Values obtained for rolling forces calculated according to Tselikov, Korolev, Sims and Siebel have a good agreement with experimentally determined values in the first six passes and eighth pass and deviations in the seventh pass. The first six passes and eighth pass have clearly expressed the contact surface and shape is closer to rolling flat profile. In the seventh pass, due to square shape, pressure on the rolls varies considerably due to uneven deformation and additional frictional force on the sides of the caliber. Values obtained for rolling forces calculated according to Ekelund, Geleji and Golovin-Tjagunov methods are too low. Based upon these results, formulae of Tselikov, Korolev, Sims and Siebel will be used in following calculation.

Because of numerous parameters (the properties of the rolls and the rolling material, the form of the grooves, the friction between rolls and rolling material, etc.) experimental methods are more suitable and more accurate for determining the rolling force in the grooves.

The obtained experimental results of rolling forces are used for the numerical analysis of local stresses by the finite element method (FEM) using ADINA software. The linear elastic model with 3D solid elements with eight nodes per element was used (Figure 7). Each node has three degrees of freedom, translation in X, Y and Z direction. Model is fixed on the both ends in the line and loaded with concentrated forces in the nodes. Figure 7 shows the concentrated force due to rolling force in pass 1.

The complete numerical analysis included 30 cases of loading according to the rolling schedule. The FEM revealed that there are three critical areas in the roll: roll neck, pass groove 3-4 and pass groove 7a. Stress concentration factors at the critical areas have a good agreement with literature (Heibach, 1989; Pilkey and Pilkey, 2008).

Figure 8 shows the FEM model of the middle roll with stock positions in pass grooves 2 and 6 and corresponding stresses in direction Z. Critical areas of the roll are marked in figure.

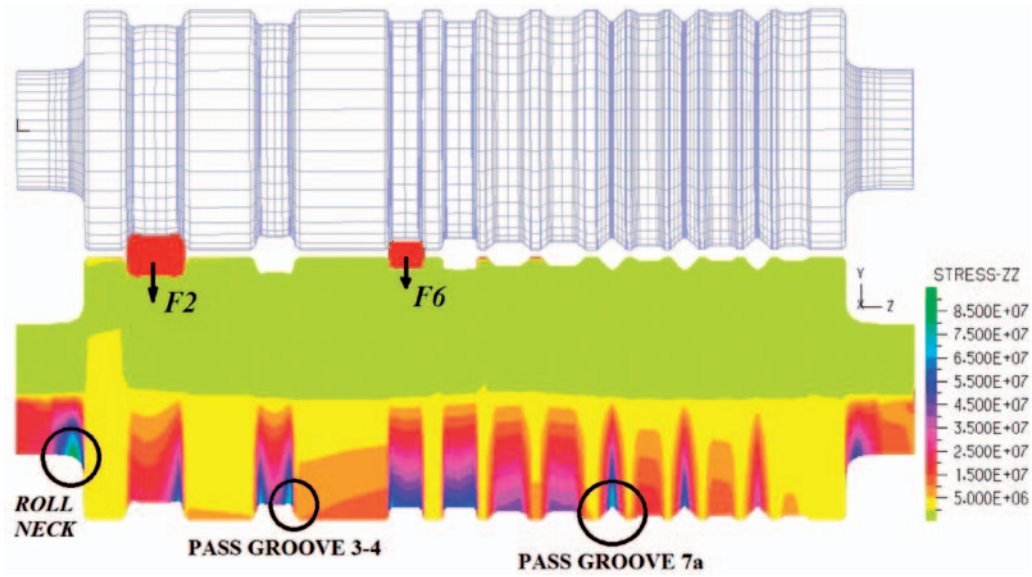

Figure 8. Numerical analysis.

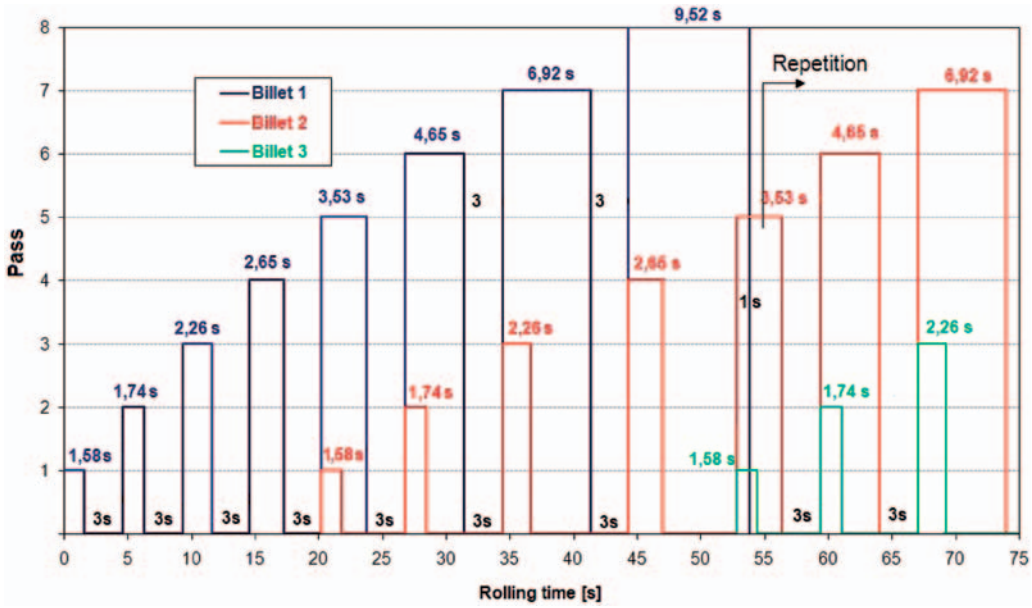

Figure 9. Rolling schedule according to time on three-high-roughing mill stand.

Three-high-roughing mill stand rolling diagram according to time is constructed from the mill production and pass schedule (Figure 9).

Rolling is starting with first billet in pass 1 and rolling duration is 1.58 s, see Figure 9. After 3 s of idle time, rolling stock is in second pass and rolling duration is 1.74 s. Then, following pass 3 and

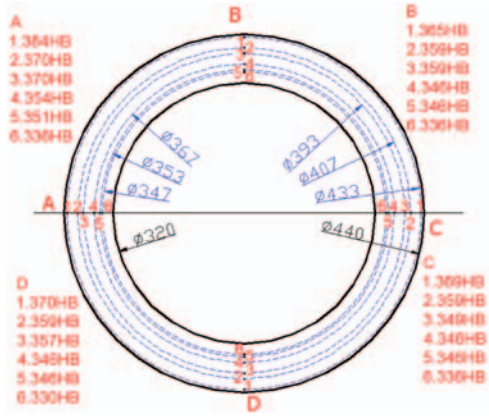

Figure 10. Ring was taken from the new roll in order to prepare specimens.

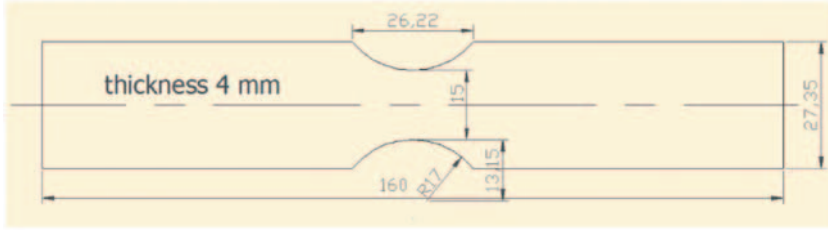

Figure 11. Shape and dimensions of the specimen.

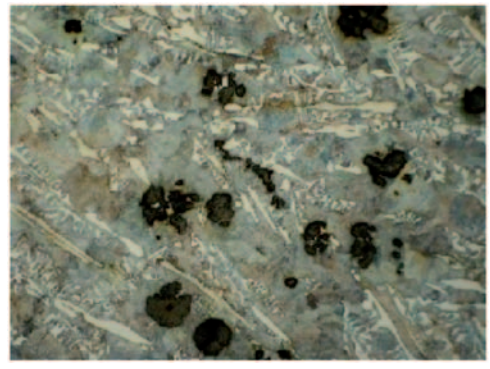

Figure 12. Metallographic structure of specimen (×500).

pass 4 and after 20 s of first stock start, the rolling process of two billets begins together. Then rolling process on the three-high-roughing mill stand continues according to rolling schedule.

Stress time histories of the individual local stress and stress spectra are obtained from numerical analysis and rolling schedule according to time (Figure 13).

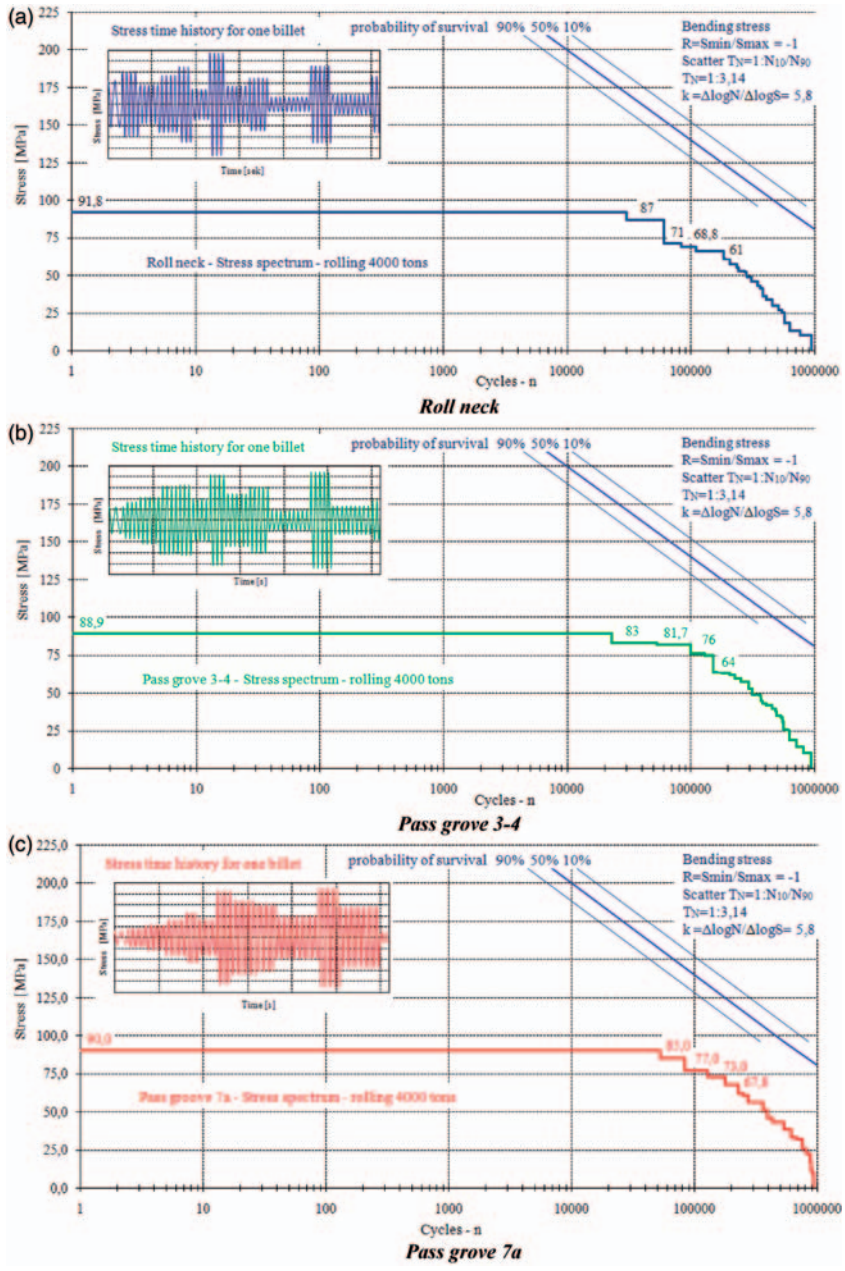

Figure 13. Stress spectra for critical areas.

Table 3. Resistance to deformation in the passes for different roll speeds.

Roll speed (r/min)	Pass No.	1	2	3	4	5	6	7	8
120	Rolling speed (ms^{-1})	2.33	2.62	2.42	2.77	2.55	2.78	2.7	2.89
120	Deformation speed (s^{-1})	7.9	9.5	7.4	12.0	9.6	15.5	10.5	18.7
120	Resistance to deformation (N/mm^2)	66.3	75.5	64.5	83	73.6	89.8	86.8	98.1
150	Rolling speed (ms^{-1})	2.92	3.28	3.03	3.46	3.19	3.47	3.38	3.61
150	Deformation speed (s^{-1})	9.9	11.9	9.2	14.9	12.0	19.4	13.1	23.4
150	Resistance to deformation (N/mm^2)	68.6	78.1	66.7	85.8	76.1	92.9	88.9	101.6
180	Rolling speed (ms^{-1})	3.50	3.93	3.63	4.15	3.83	4.17	4.06	4.33
180	Deformation speed (s^{-1})	11.8	14.3	11.0	17.9	14.4	23.2	15.7	28.1
180	Resistance to deformation (N/mm^2)	70.5	80.2	68.6	88.2	78.3	95.5	92.4	104.4

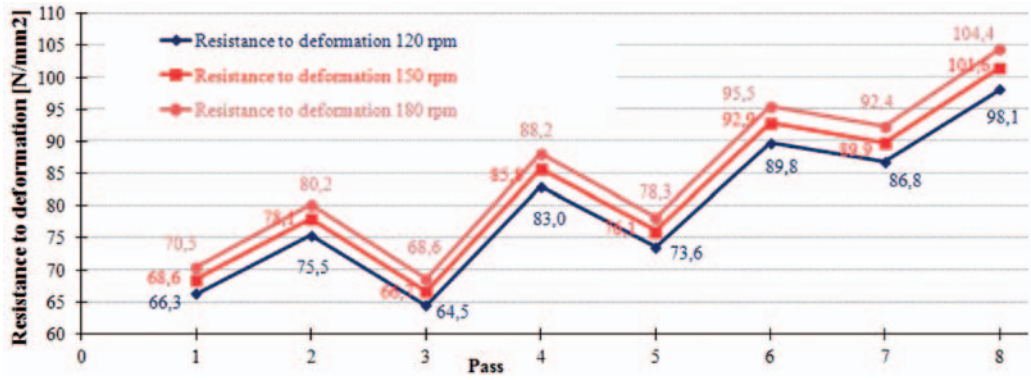

Figure 14. Influence of rolling speed on the resistance to deformation.

Fatigue strength of the roll material in the pass groove was missing, and fatigue strength was determined by experimental testing.

From the new roll dimensions ø500 × 1500 mm with same characteristic rolls in service was taken out by turning one ring dimensions ø440 × ø320 × 170 (Figure 10). The hardness measurements were done in four places.

Specimens, (as shown) in Figure 11, were taken from the ring by water cutting. Final testing shape of the specimen was made by grinding machine. During the grinding, specimens were cooled with lot of water to avoid the loss of material properties. Figure 12 shows metallographic structure of specimen.

Dynamic test was carried out in Laboratory of fatigue strength at Department of Mechanical Construction, Faculty of Electrical Engineering, Mechanical Engineering and Naval Architecture, University of Split. Bending tests were performed on the plane bending mechanical testing machine.

Figure 13 shows experimentally obtained fatigue strength of the roll material under constant amplitude in the pass groove and stress spectra of three critical areas: on the roll neck, pass groove 3-4 and pass groove 7a for 4000 rolling tons.

Table 4. Rolling forces calculation for three different roll speeds.

Roll speed (r/min)	Pass No.	1	2	3	4	5	6	7	8
120	Rolling forces Tselikov F120 (kN)	430.7	506.3	377.9	510.3	364.2	518.4	342.8	473.7
120	Rolling forces Koroljev F120 (kN)	436.0	510.5	387.8	517.2	370.4	515.2	352.3	451.6
120	Rolling forces Sims F120 (kN)	384.0	508.1	367.7	501.2	363.5	517.0	347.1	462.5
120	Rolling forces Siebel F120 (kN)	391.2	516.2	366.1	521.7	361.9	538.1	330.6	460.5
150	Rolling forces Tselikov F150 (kN)	445.4	523.6	390.9	527.9	376.8	536.3	354.7	490.3
150	Rolling forces Koroljev F150 (kN)	450.9	528.0	401.1	535.0	383.2	533.1	364.6	467.4
150	Rolling forces Sims F150 (kN)	397.2	525.5	380.3	518.5	376.1	534.9	359.2	478.7
150	Rolling forces Siebel F150 (kN)	404.6	533.9	378.7	539.7	374.4	556.8	342.1	476.6
180	Rolling forces Tselikov F180 (kN)	457.8	538.2	401.8	542.7	387.4	551.5	364.8	504.3
180	Rolling forces Korolev F180 (kN)	463.5	542.8	412.3	550.1	394.0	548.1	374.9	480.8
180	Rolling forces Sims F180 (kN)	408.2	540.1	391.0	533.0	386.6	550.0	369.4	492.3
180	Rolling forces Siebel F180 (kN)	415.8	548.8	389.3	554.8	385.0	572.5	351.8	490.2

Table 5. Force increment.

Pass No.	1	2	3	4	5	6	7	8	Average
Tselikov F_{150}/F_{120}	1.03	1.03	1.03	1.03	1.03	1.03	1.03	1.04	1.03
Koroljev F_{150}/F_{120}	1.03	1.03	1.03	1.03	1.03	1.03	1.03	1.04	1.03
Sims F_{150}/F_{120}	1.03	1.03	1.03	1.03	1.03	1.03	1.03	1.04	1.03
Siebel F_{150}/F_{120}	1.03	1.03	1.03	1.03	1.03	1.03	1.03	1.04	1.03
Tselikov F_{180}/F_{120}	1.06	1.06	1.06	1.06	1.06	1.06	1.06	1.06	1.06
Koroljev F_{180}/F_{120}	1.06	1.06	1.06	1.06	1.06	1.06	1.06	1.06	1.06
Sims F_{180}/F_{120}	1.06	1.06	1.06	1.06	1.06	1.06	1.06	1.06	1.06
Siebel F_{180}/F_{120}	1.06	1.06	1.06	1.06	1.06	1.06	1.06	1.06	1.06

From the comparison of the presented spectra it can be seen that the most critical area of the roll is pass groove 7a.

Influence of rolling speed on the rolling force

Resistance to deformation for three different roll speeds in each pass is determined from diagram of Dinnik (Figure 3). The results are shown in Table 3. The influence of rolling speed on the resistance to deformation is shown in Figure 14.

Based upon the results of experimental determination of rolling forces, the methods of Tselikov, Korolev, Sims and Siebel were used to calculate rolling forces for three different roll speeds. Values of rolling forces for three different roll speeds obtained according to these four authors are shown in Table 4.

Rolling force increments due to roll speed increasing are shown in Table 5.

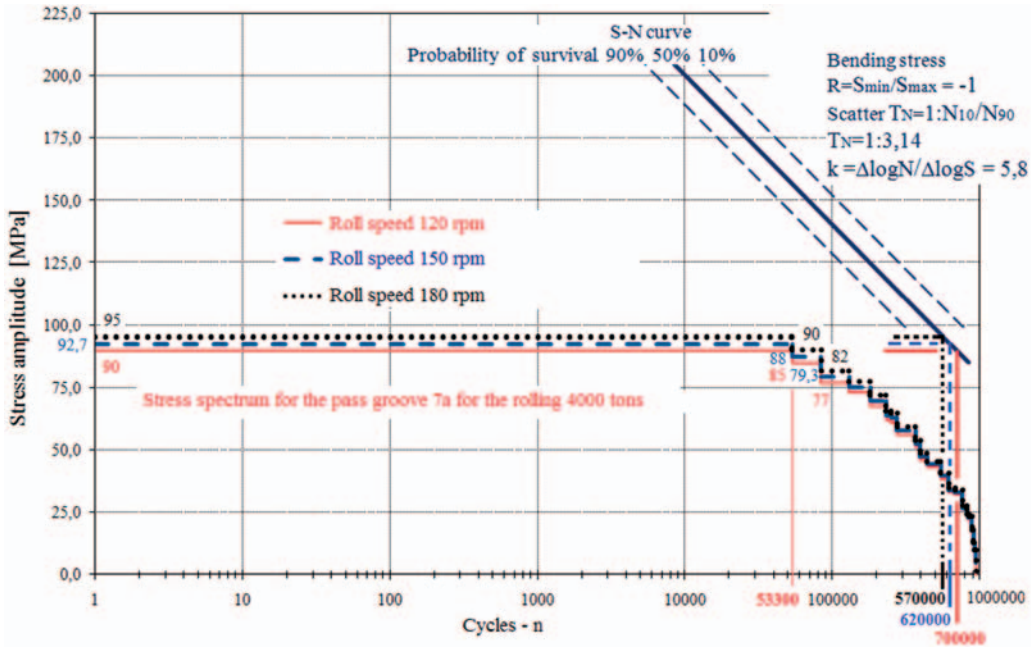

Figure 15. Influence of rolling speed on fatigue life.

Based on these data it is obvious that the increment in rolling forces is about 3% for increase in roll speed from 120 to 150 r/min and about 6% for increase in roll speed from 120 to 180 r/min.

Results and discussion

The obtained experimental values of rolling forces with an increase of 3% and 6% are used for numerical analysis of local stresses by the FEM. Stress spectra for the roll speeds 150 and 180 r/min determined from numerical analysis and rolling schedule according to time are shown in Figure 15.

From Figure 15 it is evident that:

- Increase in rolling speed from 120 to 150 r/min causes increase in rolling force by 3% and reduces the fatigue life of the roll for about 11%.
- Increase in rolling speed from 120 to 180 r/min causes increase in rolling force by 6% and reduces the fatigue life of the roll for about 19%.
- Although increase in rolling speed which causes decrease in the fatigue life of the roll, the stresses caused by rolling with increasing speed for 50% should not lead to roll fracture for the rolling 4000 tons.

Conclusions

The analysis of rolling speed effects on calibrated rolls fatigue life shows that maximum increase in rolling speed inside the technological limits will not affect the roll fatigue life and increase in overall production by increasing the rolling speed should not lead to roll fracture.

References

Čaušević M (1979) *Teorija Plastične Prerade Metala*. Sarajevo: Svjetlost.

Čaušević M (1983) *Obrada Metala Valjanjem*. Sarajevo: Veselin Masleša.

Designs and technological rules "*Steelworks Split*". Croatia: Kaštel Sućurac.

Domazet Ž and Lukša F (2005) Experimental determination of the rolling force on the rolls with grooves. In: *Proceedings of the 22-nd symposium "DANUBIA-ADRIA" on experimental methods in solid mechanics*, Parma, Italy.

Domazet Ž, Lukša F and Šušnjar M (2007) Failure analysis of rolls with grooves. *Engineering Failure Analysis* 14(6): 1116–1174.

Heibach E (1989) *Betriebfestigkeit*. Düseldorf: VDI Verlag Gmbh.

Lukša F (2005) *Investigation of the cause of the failures of the rolls with grooves*. Master Thesis, University of Split, Croatia.

Lukša F (2013) *Methodology of constructing optimal calibrated rolls with respect to fatigue strength*. PhD Thesis, University of Split, Croatia.

Pilkey WD and Pilkey DF (2008) *Stress Concentration Factors*, 3rd ed. Hoboken, NJ: John Wiley & Sons.